# Observations of the boundary currents and AMOC at 11˚S - the TRACOS array

R. Hummels[1], P. Brandt[1,2], M. Dengler[1], R. Imbol Koungue[1], A. C. Hans[1]

[1] GEOMAR Helmholtz Centre for Ocean Research Kiel
[2] Faculty of Mathematics and Natural Sciences, Kiel University, Kiel, Germany

## Introduction

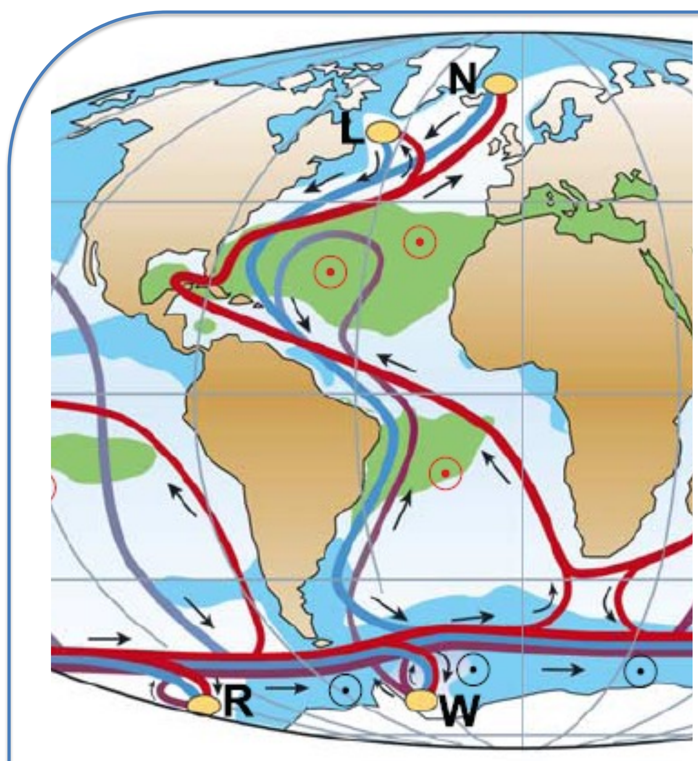

*Fig. 1: Sketch of the AMOC from Kuhlbrodt et al. 2007. Warm surface flows in in red, cold deep flows in blue. The letters mark areas of deep water formation.*

***The upper-ocean circulation of the tropical Atlantic is a complex superposition of thermohaline and wind-driven flows. The zonally and vertically integrated upper-ocean meridional flow is associated with the upper branch of the Atlantic Meridional Overturning Circulation (AMOC) — a major component of the global climate system (Fig. 1). In the tropics, the northward AMOC flow is superimposed by the shallower overturning associated with the wind-driven Subtropical cells (STCs, Fig. 2). One of the key regions in the tropical Atlantic is the western boundary current system off Brazil. This region serves as a crossroads for the meridional transfer of mass, heat, and salt between the Northern and Southern hemisphere.***

***The TRACOS (TRopical Atlantic Circulation & Overturning at 11°S) array consists of four tall moorings at the western boundary and of formerly two and nowadays one tall mooring at the eastern boundary. Pressure Inverted Echo Sounders on both sides of the basin as well as all other available data sets provide a comprehensive data set at 11°S.***

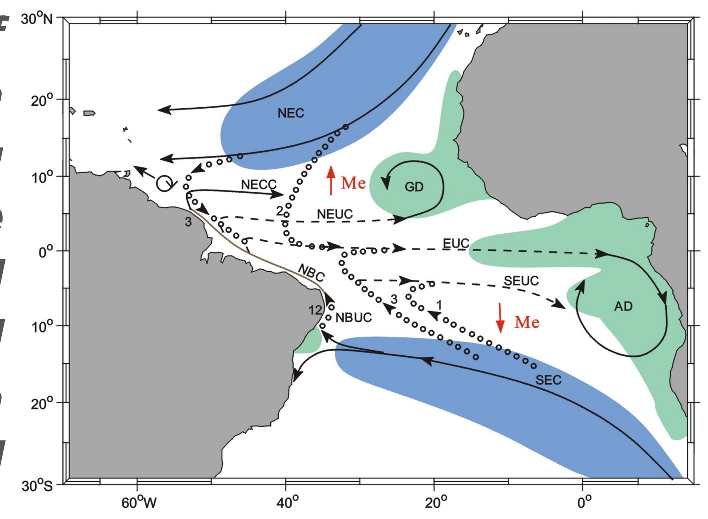

*Fig. 2: Sketch of the Atlantic Subtropcial Cells from Schott et al. 2004. Blue/green shading mark subduction/upwelling areas. Me (red) indicates Ekman flow. Abbreviations stand for individual current branches.*

## Western Boundary (WB)

The warm water return path of the AMOC and STCs is concentrated in the North Brazil Under Current (NBUC). The cold water path of the Deep Western Boundary current (DWBC) breaks up into eddies at about 8˚S (Fig, 3, 4).

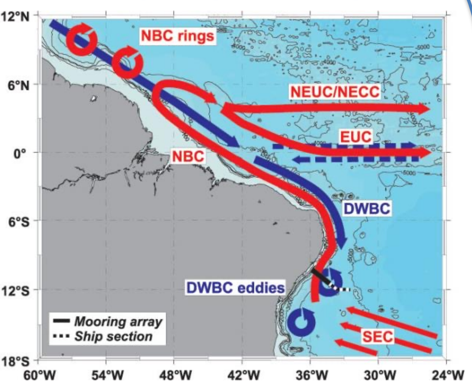

*Fig. 3: Sketch of flow pathways and mooring locations at the WB from Dengler et al. 2004.*

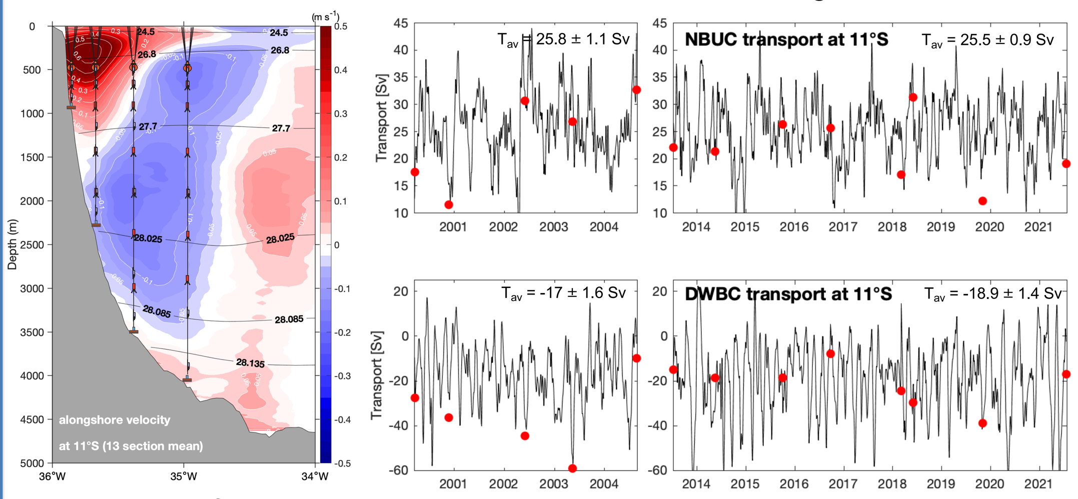

*Fig. 4: Left: Mean alongshore velocity with mooring array design superimposed. Right: Transport time series of the NBUC (top panels) and DWBC (lower panels). Red dots indicate ship section transports. Update from Hummels et al. 2015.*

- both flow components are rather stable in their characteristics (Fig. 4)
- deep eddies are still clearly present (Fig. 4)
- salinity increase in central water range (not shown) likely linked to Agulhas leakage increase

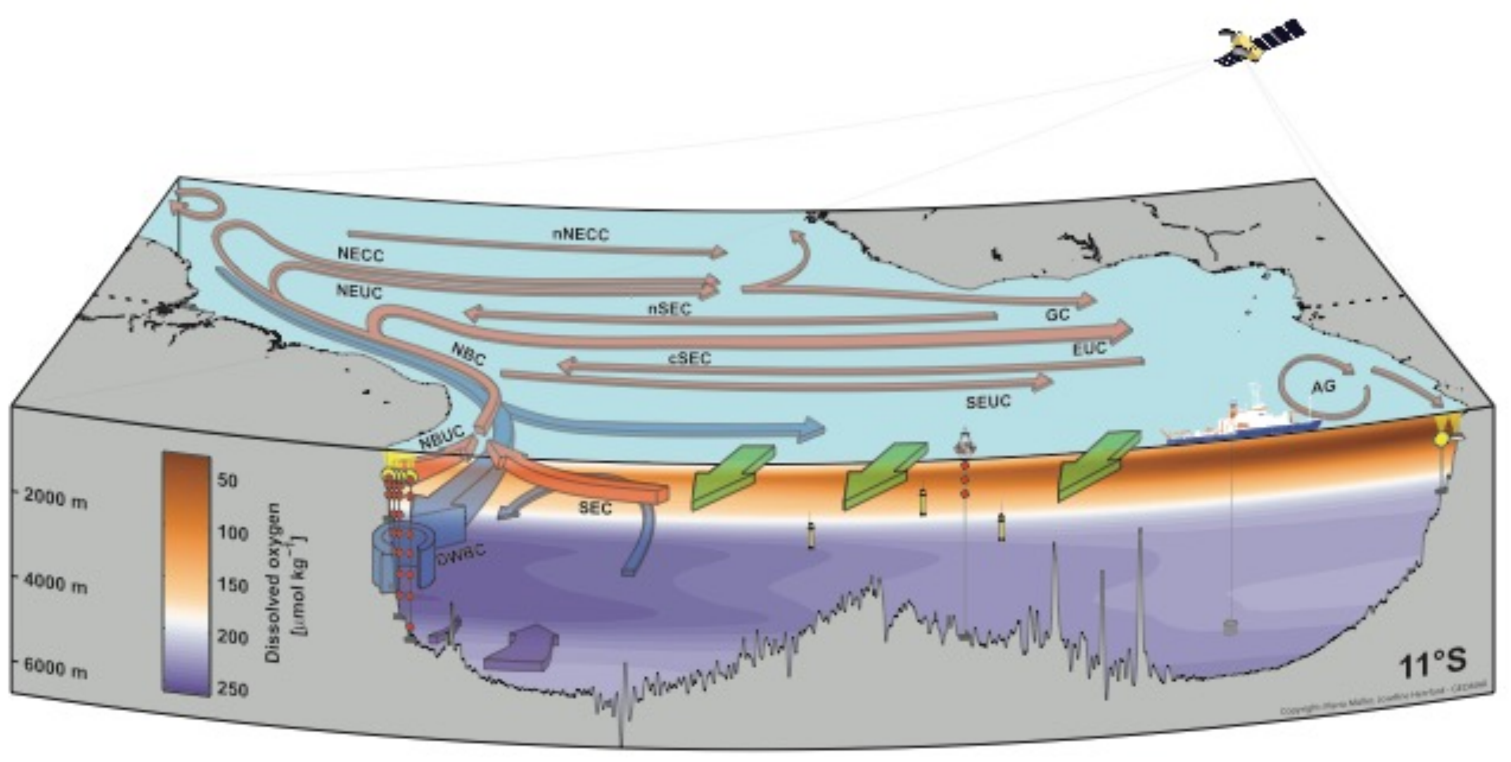

### The TRACOS observing system at 11˚S

- **WB mooring array** *(Dengler et al., 2004, Schott et al., 2005; Hummels et al., 2015)*
- **EB mooring(s)** *(Kopte et al., 2017, 2018, Imbol Koungue et al. 2021a,b)*
- **Bottom pressure recorders (BPR)** *(Herrford et al.2021, Chidichimo et al. 2023)*
- **Ship-based measurements** (German cruises/ PIRATA cruises/Brazilian Navy/EAF-Nansen program)
- **SLA, Argo & wind products (**Tuchen et al. 2019, 2022)

## Eastern Boundary (EB)

At the EB, 11˚S is located in an upwelling system, where seasonally sea surface temperatures drop and nutrients are brought into the euphotic zone sustaining a highly productive ecosystem.

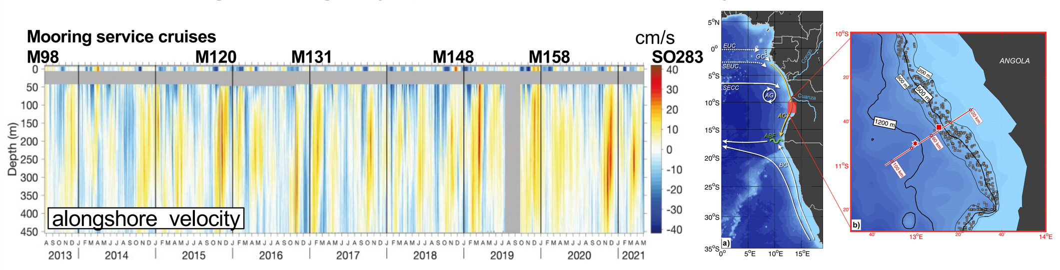

*Fig. 5: Left: Alongshore flow of the Angola current. Right: Location of the mooring(s). Update from Kopte et al. 2017.*

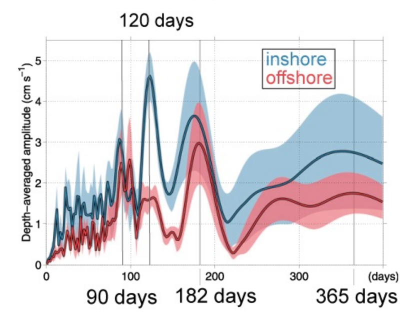

*Fig. 6: Mean periodograms of alongshore velocity (Kopte et al. 2018).*

- weak mean alongshore flow of 5-8 cm/s (Fig. 5)
- distinct spectral peaks at the annual, semi-annual and intra-seasonal period (Fig. 6)

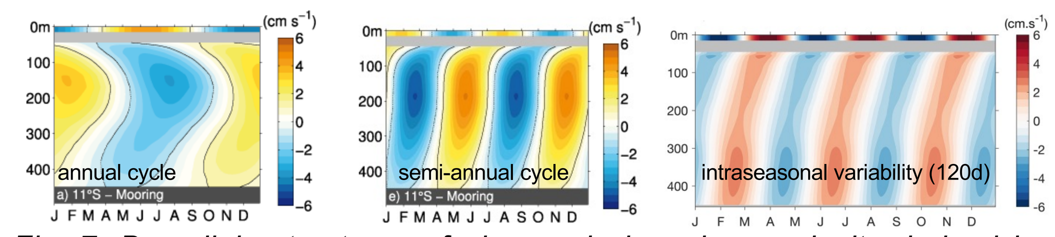

*Fig. 7: Baroclinic structures of observed alongshore velocity derived by fitting harmonic functions at each depth level for different periods (Left & middle Kopte et al. 2018, right Imbol Koungue and Brandt 2021).*

- assessed variability patterns at 11˚S fit to variability patterns forced in the equatorial region
  - signals travel to 11˚S via wave dynamics

## AMOC strength and variability at 11˚S

AMOC variability is assessed as combination of bottom pressure data on both sides of the basin at 300 and 500m depth, sea-level anomaly (SLA) as well as wind data from satellite observations (Herrford et al. 2021).

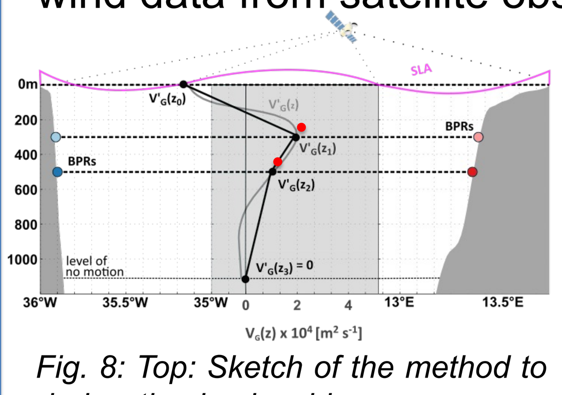

$$V'_G(z,t) = \frac{P'_{EB}(z,t) - P'_{WB}(z,t)}{\rho_0 \cdot f}$$

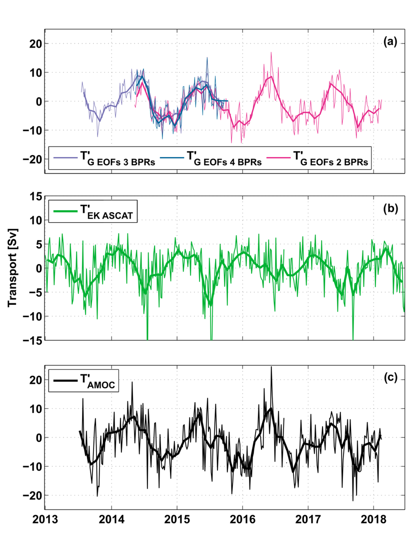

*Fig. 8: Top: Sketch of the method to derive the basin-wide upper ocean geostrophic transport anomaly. Right: Anomaly time series of geostrophic transport (top), Ekman transport from ASCAT winds (middle) and the resulting AMOC transport (bottom) from Herrford et al. 2021.*

- geostrophic transport anomaly per unit depth determined from pressure anomaly difference (Fig. 8, 9)
- AMOC anomaly time series at 11˚S strongly dominated by seasonal time scale (Fig. 9)
- uncertainties in wind strongly relevant for AMOC uncertainties
- pressure anomalies from both boundaries contribute to seasonal cycle

The strength of the AMOC return flow in the upper 1200m can be estimated from Argo and wind data (Tuchen et al. 2022).

- high resolution Argo product agrees well at the WB in terms of structure and transports with shipboard observations (Fig. 9, 10)

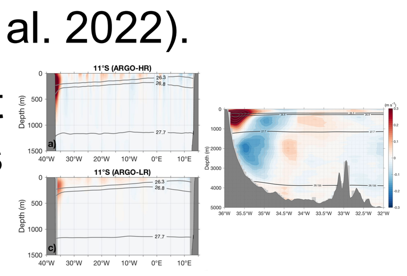

*Fig. 9: Boundary current structure from Argo (geostrophic) and shipboard observations*

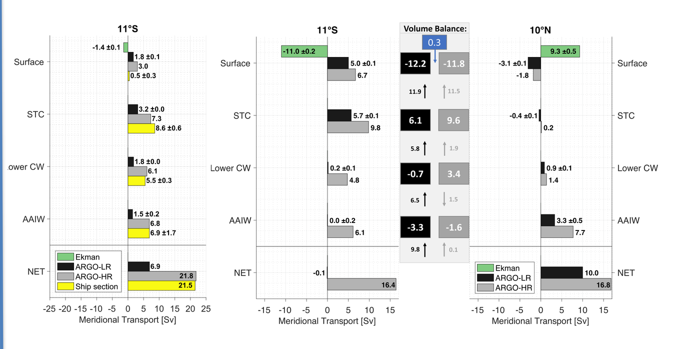

*Fig. 10: Meridional (geostrophic) volume transports in different density layers at the WB at 11˚S (left), across the basin at 11˚S (middle) and at 10˚N (right) based on Argo data from Tuchen et al. 2022.*

- AMOC strength at 11˚S and 10˚N of 16-17 Sv (Fig. 10)
- diapycnal transport from central water into thermocline layer ~ 2 Sv (Fig. 10)
- at 11˚S transport is concentrated at the WB, while at 10°N only ~60% of the flow takes boundary route

Together, the AMOC anomaly time series (left side) and the mean AMOC strength (middle panel) provide the first AMOC estimate at 11˚S (Fig. 11).

- Contribution to SAMOC
- Comparison to other latitudes, but what do we expect to see?

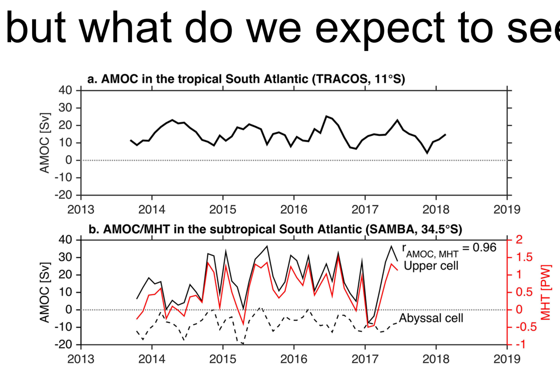

*Fig. 11: (S)AMOC time series at 11˚S (top) and 34.5˚S (bottom) from Chidichimo et al. 2023.*

**References**

Chidichimo, M.P., Perez, R.C., Speich, S., M. Kersalé, J. Sprintall, S. Dong, T. Lamont, O. T. Sato, T. K. Chereskin, **R. Hummels** & C. Schmid (2023), Energetic overturning flows, dynamic interocean exchanges, and ocean warming observed in the South Atlantic, Communications Earth & Environment, in press, doi: doi:10.1038/s43247-022-00644-x.

**Dengler, M**., F. A. Schott, C. Eden, **P. Brandt**, J. Fischer & R. J. Zantopp (2004), Break-up of the Atlantic deep western boundary current into eddies at 8° S, Nature, 432(7020), 1018-1020, doi: 10.1038/nature03134.

Herrford, J., **P. Brandt**, T. Kanzow, **R. Hummels**, M. Araujo, and J. V. Durgadoo (2021), Seasonal variability of the Atlantic Meridional Overturning Circulation at 11° S inferred from bottom pressure measurements, Ocean Sci., 17(1), 265-284, doi: 10.5194/os-17-265-2021.

**Hummels, R., P. Brandt**, **M. Dengler**, J. Fischer, M. Araujo, D. Veleda, and J. V. Durgadoo (2015), Interannual to decadal changes in the western boundary circulation in the Atlantic at 11° S, Geophysical Research Letters, 42(18), 7615-7622, doi: https://doi.org/10.1002/2015GL065254.

**Imbol Koungue, R. A**., & **Brandt, P.** (2021). Impact of intraseasonal waves on Angolan warm and cold events. Journal of Geophysical Research: Oceans, 126, e2020JC017088. https://doi.org/10.1029/2020JC017088

Kopte, R., **Brandt, P.**, **Dengler, M.,** Tchipalanga, P. C. M., Macuéria, M., and Ostrowski, M. (2017), The Angola Current: Flow and hydrographic characteristics as observed at 11° S, J. Geophys. Res. Oceans, 122, 1177– 1189, doi:10.1002/2016JC012374.

Kopte, R., **P. Brandt**, M. Claus, R. J. Greatbatch, and **M. Dengler** (2018): Role of Equatorial Basin-Mode Resonance for the Seasonal Variability of the Angola Current at 11° S. J. Phys. Oceanogr., 48, 261–281, https://doi.org/10.1175/JPO-D-17-0111.1.

SAMOC program, https://www.aoml.noaa.gov/phod/SAMOC_international/

Schott, F.A., Mccreary, J.P., Jr. and Johnson, G.C. (2004). Shallow Overturning Circulations of the Tropical-Subtropical Oceans. In Earth's Climate (eds C. Wang, S.P. Xie and J.A. Carton). https://doi.org/10.1029/147GM15

Schott, F. A., **M. Dengler**, R. Zantopp, L. Stramma, J. Fischer, and **P. Brandt** (2005), The shallow and deep western boundary circulation of the South Atlantic at 5–11 S, Journal of Physical Oceanography, 35(11), 2031-2053, doi: https://doi.org/10.1175/JPO2813.1.

Tuchen, F. P., **P. Brandt**, J. F. Lübbecke, and **R. Hummels** (2022), Transports and Pathways of the Tropical AMOC Return Flow From Argo Data and Shipboard Velocity Measurements, Journal of Geophysical Research: Oceans, 127(2), e2021JC018115, doi: https://doi.org/10.1029/2021JC018115.

## What's next?

- Next WB/EB cruise proposed for winter/spring 2025
- Prolong all time series WB, EB and AMOC based on moorings and bottom pressure and analyse them on different time scales
- Try other AMOC estimates based on various other data products specifically focusing on the interior part (Argo, SSH, etc.)
  - Get a comprehensive AMOC estimate at 11˚S
  - Relate assessed AMOC variability to tropical Atlantic variability
  - Possibly compare (partly) to other latitudes